An insight into charge-transfer transitions and their band widths: analysis of $Na_3In_2Li_3F_{12} : Cr^{3+}$

An insight into charge-transfer transitions and their band widths: analysis of $Na_3In_2Li_3F_{12}$:Cr^{3+}

J A Aramburu†, M T Barriuso‡ and M Moreno†

† Departamento de Ciencias de la Tierra y Física de Materia Condensada, Facultad Ciencias, Universidad de Cantabria, 39005 Santander, Spain
‡ Departamento de Física Moderna, Facultad de Ciencias, Universidad de Cantabria, 39005 Santander, Spain

Abstract. Spin-polarized MS–Xα and self-consistent charge extended Hückel calculations on CrF_6^{3-} as a function of the Cr–F$^-$ distance R have been carried out in order to clarify the origin of the bands detected in the vacuum ultraviolet excitation spectrum of $Na_3In_2Li_3F_{12}$: Cr^{3+} associated with charge-transfer (CT) transitions as well as what electronic orbitals are involved in the jump. With the help of results on other 3d impurities it is explained that the two first transitions peaked at 8.0 and 8.7 eV are the $t_{1u}(\sigma - \pi) \uparrow \rightarrow e_g^* \uparrow$ and $t_{1u}(\sigma + \pi) \uparrow \rightarrow e_g^* \uparrow$ CT transitions while other transitions involving at least one-orbital *without* σ bonding would display a smaller oscillator strength. It is shown that the two referred transitions both exhibit a strong dependence on R ($\partial E/\partial R$ being about -200 meV pm^{-1}) whose microscopic origin is explained. Using this R dependence an explanation of the experimental band width W of a CT transition is attempted for the first time. The present analysis indicates that W can be understood simply considering the coupling with the A_{1g} mode, leading to a Huang–Rhys factor $S = 20$. Also it is pointed out that CT transitions involving the t_{2g}^* orbital would give rise to a significant decrement in S.

The present results together with experimental data on other 3d complexes indicate that the $\gamma_L \downarrow \rightarrow e_g^* \downarrow$ transitions (where γ_L is $t_{1u}(\sigma - \pi)$ and $t_{1u}(\sigma + \pi)$) are probably contained in the broad third band peaked at 12 eV. Also they shed some light on the experimental results of other systems such as Al_2O_3 : Ti^{4+} and Cs_2NaYCl_6 : Fe^{3+} which are briefly discussed.

1. Introduction

Part of the research on solid state lasers requires an understanding of the microscopic origin of optical properties for insulating lattices (such as fluorides or oxides) doped with transition-metal impurities. Although the charge-transfer (CT) bands corresponding to transition-metal complexes with O_h symmetry are much more intense than those due to crystal-field transitions, more attention has been paid to the latter than to the former. Therefore questions on CT transitions such as the assignment and relative intensities of the observed bands, the actual values of Huang–Rhys factors or the microscopic origin of the band widths are far from being answered.

In halide host lattices, studies exploring the CT bands of 3d and 4d impurities in fluorides are particularly scarce as, in general, they appear outside the optical spectrum region, in the so-called vacuum ultraviolet region [1]. Recently [2], the advent of synchrotron radiation facilities has allowed the excitation spectrum of $Na_3In_2Li_3F_{12}$: Cr^{3+} to be observed up to photon energies of 30 eV.
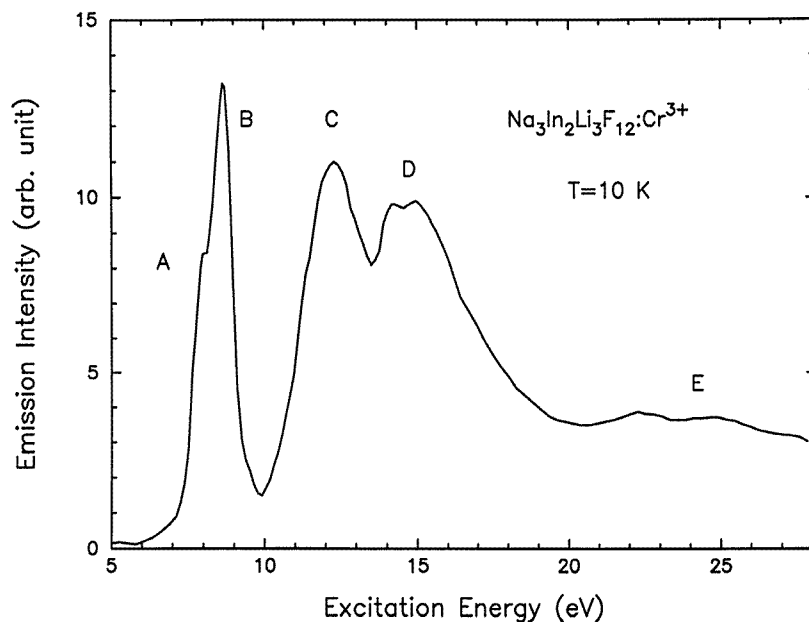
Figure 1. Experimental excitation spectrum at $T = 10$ K of Na$_3$In$_2$Li$_3$F$_{12}$: Cr^{3+} in the 5–30 eV range. This figure is reprinted from de Viry *et al* [2] published (copyright 1990) with kind permission from Elsevier Science Ltd.

The experimental spectrum reported by de Viry *et al* [2] in the region 5 eV $< E <$ 30 eV is given in figure 1. This excitation spectrum has been corrected so that the experimental band widths are meaningful. An account of the experimental details can be found in the article by de Viry *et al* [2]. The first two bands (A and B) of such a spectrum have maxima at $E_A = 8.0$ eV and $E_B = 8.7$ eV. Within the experimental uncertainty, both exhibit [2] a *full band width* $W = 0.7$ eV at $T = 10$ K. Above $E_B = 8.7$ eV, there is a gap until band C (figure 1) is reached whose maximum is located at $E_C = 12.0$ eV and whose full band width is equal to $W_C = 1.5$ eV.

De Viry *et al* have suggested that bands A and B can be CT transitions of the CrF$_6^{3-}$ complex based on Jørgensen's [1] optical electronegativity scale. De Viry *et al* are uncertain whether bands A and B can be described as $\gamma_L^6 t_{2g}^{*3} \rightarrow \gamma_L^5 t_{2g}^{*4}$ or $\rightarrow \gamma_L^6 t_{2g}^{*3} \rightarrow \gamma_L^5 t_{2g}^{*3} e_g^*$ CT excitations where γ_L is a bonding t$_{1u}$ orbital (mainly built from 2p(F$^-$) orbitals of ligands) or a non-bonding t$_{2u}$ orbital. As usual t$_{2g}^*$ and e$_g^*$ denote the antibonding (mainly 3d) orbitals of the CrF$_6^{3-}$ complex. Bands C and D are assigned [2] to intra-atomic 3d $\rightarrow$ 4s transitions although they display similar intensities to those of bands A and B in the excitation spectrum in figure 1.

The first goal of the present work is to clarify the origin of the spectrum of figure 1 by undertaking theoretical calculations on the CT transitions of the CrF$_6^{3-}$ complex at different values of the Cr^{3+}–F$^-$ distance R. It is worth noting that, in the excitation spectrum associated with the well characterized emission spectrum of CrF$_6^{3-}$, bands due to *other* impurities or the host lattice can *also* appear provided that an energy *transfer* process between such entities and CrF$_6^{3-}$ takes place.

In addition to confirming that the maxima seen in figure 1 are related to CT transitions,

particular attention is addressed to the dependence $E(R)$ of a CT transition energy on the distance R and to the assignment. This point is of particular importance as the experimental [3] and theoretical [4] studies on CT transitions of d^9 ions show that they are certainly sensitive to R variations. Therefore the concept of optical electronegativity should be viewed only as approximately valid. Moreover, taking into account the dependence $E(R)$ found in the calculations, we shall attempt to explain the experimental band widths following the theoretical framework given in [4].

To achieve all these goals, self-consistent charge extended Hückel (SCCEH) and spin-polarized MS–Xα calculations employing the Norman [5] criterion on the CrF_6^{3-} unit have been performed. For the assignment of bands, first results on the oscillator strengths of CT transitions on d^9 impurities have also been taken into account [6, 7]. In previous studies of optical and EPR properties of 3d impurities the SCCEH and the MS–Xα methods have both led to a reasonable understanding of the experimental parameters [4, 6]. This is particularly true for CT transitions where *ab-initio* methods using a moderate-quality basis can lead to a poor description of CT transitions [8, 9] because of an underestimation of the electronic affinity of halides. This situation appears for instance in the calculation of [9] on CrF_6^{3-} where the mainly 2p(F^-) ligand levels lie *above* the mainly 3d levels of Cr^{3+}. It is worth noting that the methods used in this work are suitable for describing transitions involving orbitals of the complex, but not for studying transitions such as those arising from the 3d $\rightarrow$ 4s or 3d $\rightarrow$ 4p of central cation. In fact, the levels arising from atomic 4s or 4p orbitals are more diffuse (as they lie close to the conduction band of the host lattice) and thus an accurate study of them usually requires calculations on clusters larger than CrF_6^{3-} to be undertaken.

The present calculations have been performed in the 185 pm $\leqslant R \leqslant$ 195 pm range because equilibrium R-values for CrF_6^{3-} appear at around $R = 190$ pm. In particular, recent x-ray measurements on the Rb_2KCrF_6 compound give $R = 188$ pm [10]. To check the MS–Xα and SCCEH methods in the present case we have calculated the $10Dq$-value. At $R = 190$ pm both methods give $10Dq \simeq 16.000$ cm^{-1} which is in agreement with the experimental values found for Cr^{3+}-doped $Na_3In_2Li_3F_{12}$ and fluoroelpasolites [9, 11–14]. More details on the calculations have been given in [4, 6].

2. Results

2.1. Assignment of bands

The ground state of the CrF_6^{3-} complex can simply be written as $\gamma_L^6 t_{2g}^{*3}$ and has $S = 3/2$. On going from the ground state to an excited CT state, an electron jumps from a mainly ligand level γ_L (with an one-electron energy ϵ_L) to a mainly 3d orbital whose one-electron energy is denoted as ϵ_M. An allowed CT transition can thus be described as $\gamma_L^6 t_{2g}^{*3} \rightarrow \gamma_L^5 t_{2g}^{*m} e_g^{*n}$ (S'). Here S' denotes the spin of the 3d subshell [1] formed by all the electrons placed in the antibonding t_{2g}^* and e_g^* orbitals and can take a value $S' = 2$ or 1. In the case of m and n, there are two possibilities: either $m = 4$, $n = 0$ and $S' = 1$, or $m = 3$, $n = 1$ and then $S' = 2$ or $S' = 1$.

The excitation energy E involved on passing from the ground (g) to the excited (e) CT state depends not only on $\epsilon_M - \epsilon_L$ but also on the so-called spin-pairing effects in the 3d subshell [1]. Therefore, to calculate E from the SCCEH results, one has to use the following expression:

$$E = \epsilon_M - \epsilon_L + E_{SP}(e) - E_{SP}(g). \tag{1}$$

The spin-pairing energy E_{SP} associated with a $t_{2g}^{*m} e_g^{*n}$ (S') configuration is given by [1]

$$E_{SP} = D\{\langle S'(S'+1)\rangle - S'(S'+1)\}$$

$$\langle S'(S'+1)\rangle = \frac{3}{4}q\left(1 - \frac{q-1}{9}\right) \qquad (q = m + n) \qquad (2)$$

$$D = \tfrac{7}{6}(\tfrac{5}{2}B + C)$$

where B and C are the effective Racah parameters. From the optical data [11] on $Na_3In_2Li_3F_{12} : Cr^{3+}$, it has been found that $B = 90$ meV and $C = 410$ meV for CrF_6^{3-}. Therefore D in (2) is derived to be equal to 745 meV. Similar values of D are found from the analysis of optical spectra [12, 15] corresponding to $K_2NaGaF_6 : Cr^{3+}$ or $RbCaF_3 : Cr^{3+}$. It is worth noting that the theoretical results [16] on CrF_6^{3-} as well as experimental [17] and theoretical [8] studies on MnF_6^{4-} demonstrate that the effective Racah parameters B and C are nearly independent of the metal–ligand distance R.

Table 1. Energies corresponding to different electric dipole allowed CT transition of CrF_6^{3-} computed at different values of the Cr^{3+}–F^- distance R through the SCCEH method. The CT transitions are characterized by i → f where i and f denote the 'initial' and 'final' orbital involved in the electron jump as well as by the S'-value in the excited state. The values of $\epsilon_M - \epsilon_L$ are given in the first rows and the corresponding excitation energies E according to (1) are given in the second rows.

Transition		$R = 185$ pm	$R = 191$ pm	$R = 195$ pm
$t_{1u}(\sigma - \pi) \rightarrow e_g^*$ ($S' = 2$)	$\epsilon_M - \epsilon_L$ (eV)	9.64	8.35	7.59
	E (eV)	8.15	6.86	6.10
$t_{1u}(\sigma - \pi) \rightarrow t_{2g}^*$ ($S' = 1$)	$\epsilon_M - \epsilon_L$ (eV)	7.34	6.43	5.88
	E (eV)	8.83	7.92	7.37
$t_{2u} \rightarrow e_g^*$ ($S' = 2$)	$\epsilon_M - \epsilon_L$ (eV)	9.78	8.45	7.68
	E (eV)	8.29	6.96	6.19
$t_{1u}(\sigma + \pi) \rightarrow e_g^*$ ($S' = 2$)	$\epsilon_M - \epsilon_L$ (eV)	10.07	8.69	7.88
	E (eV)	8.58	7.20	6.39
$t_{1u}(\sigma + \pi) \rightarrow t_{2g}^*$ ($S' = 1$)	$\epsilon_M - \epsilon_L$ (eV)	7.78	6.77	6.18
	E (eV)	9.27	8.26	7.67
$t_{1u}(\sigma - \pi) \rightarrow e_g^*$ ($S' = 1$)	$\epsilon_M - \epsilon_L$ (eV)	9.64	8.35	7.59
	E (eV)	11.15	9.84	9.08
$t_{1u}(\sigma + \pi) \rightarrow e_g^*$ ($S' = 1$)	$\epsilon_M - \epsilon_L$ (eV)	10.07	8.69	7.88
	E (eV)	11.56	10.20	9.37

Table 1 shows the calculated values E of several CT excitations, using the SCCEH method and spin-pairing corrections given in (2). In table 2, similar results derived from the polarized MS–Xα method are given using the transition state where spin-pairing effects are automatically included. The mainly ligand levels involved in an allowed CT jump can be [18] $t_{1u}(\sigma - \pi)$, and $t_{1u}(\sigma + \pi)$, or/and t_{2u}. In the levels called $t_{1u}(\sigma - \pi)$ and $t_{1u}(\sigma + \pi)$, a linear combination of σ and π orbitals made through $2p(F^-)$ orbitals of the six ligands is involved. Such a linear combination displays a ligand–ligand antibonding character for the $t_{1u}(\sigma - \pi)$ orbital but a bonding character for $t_{1u}(\sigma + \pi)$. Thus the energy associated with

Table 2. Energy of CT transitions of CrF$_6^{3-}$ calculated using the polarized MS–Xα method on transition states for different R-values. The transitions depicted as t$_{1u}(\sigma - \pi)$ ↑→ e$_g^*$ ↑ and t$_{1u}(\sigma - \pi)$ ↓→ e$_g^*$ ↓ in the present scheme correspond to t$_{1u}(\sigma - \pi) \rightarrow$ e$_g^*$ ($S' = 2$) and t$_{1u}(\sigma - \pi) \rightarrow$ e$_g^*$ ($S' = 1$) respectively, in table 1.

	E (eV)		
Transition	$R = 185$ pm	$R = 191$ pm	$R = 195$ pm
t$_{1u}(\sigma - \pi)$ ↑→ e$_g^*$ ↑	9.81	8.49	7.76
t$_{1u}(\sigma - \pi)$ ↓→ t$_{2g}^*$ ↓	10.38	9.52	9.00
t$_{2u}$ ↑→ e$_g^*$ ↑	10.16	8.75	7.98
t$_{1u}(\sigma + \pi)$ ↑→ e$_g^*$ ↑	11.04	9.60	8.80
t$_{1u}(\sigma + \pi)$ ↓→ t$_{2g}^*$ ↓	11.55	10.57	9.97
t$_{1u}(\sigma - \pi)$ ↓→ e$_g^*$ ↓	11.8	10.42	10.00
t$_{1u}(\sigma + \pi)$ ↓→ e$_g^*$ ↓	12.95	11.50	11.02

t$_{1u}(\sigma - \pi)$ is higher than that for t$_{1u}(\sigma + \pi)$. Inspection of tables 1 and 2 shows that the lowest excitation energy E corresponds to the t$_{1u}(\sigma - \pi) \rightarrow$ e$_g^*$ ($S' = 2$) transition (called t$_{1u}(\sigma - \pi)$ ↑→ e$_g^*$ ↑ in the polarized MS–Xα framework) and not to the t$_{1u}(\sigma - \pi) \rightarrow$ t$_{2g}^*$ ($S' = 1$) (designed as t$_{1u}(\sigma - \pi)$ ↓→ t$_{2g}^*$ ↓ in the polarized MS–Xα method). This reflects the decrement in the total energy produced by pairing the four electrons in the d subshell with the same spin, a fact which can occur in the t$_{2g}^{*3}$e$_g^{*1}$ configuration but never in the t$_{2g}^{*4}$. In other words, the gain in spin pairing energy ($4D$) can balance the increase ($10Dq$) induced by transferring the electron to a higher one-electron orbital.

Moreover, the values obtained for the t$_{1u}(\sigma - \pi)$ ↑→ e$_g^*$ ↑ transition (for R close to 190 pm) are not far from the experimental value $E_A = 8.0$ eV measured for peak A in figure 1. Nevertheless, tables 1 and 2 indicate that the transitions γ_L ↓→ t$_{2g}^*$ ↓ and γ_L ↑→ e$_g^*$ ↑, where γ_L is a t$_{1u}(\sigma - \pi)$, t$_{2u}$ or t$_{1u}(\sigma + \pi)$ orbital, lie within about 1 eV. By contrast, in the range 8–9 eV, only *two* peaks (instead of six) are clearly distinguished in the experimental spectrum displayed in figure 1. This puzzling situation can, however, be clarified by taking into account the results reached on oscillator strengths corresponding to CT transitions of d^9 ions. In fact, it has been shown that, among the dipole-allowed CT transitions, those involving $|i\rangle \rightarrow |f\rangle$ jumps where *both* $|i\rangle$ and $|f\rangle$ are σ orbitals have oscillator strengths which are higher than the others [6, 7]. As among the six considered excitations only the *two* t$_{1u}(\sigma - \pi)$ ↑→ e$_g^*$ ↑ and t$_{1u}(\sigma + \pi)$ ↑→ e$_g^*$ ↑ transitions follow this rule, the two peaks A and B seen experimentally can be ascribed mainly to such transitions.

The separation Δ between such transitions is around 1.1 eV for the MS–Xα calculation but equal to 0.4 eV for the SCCEH calculation. The experimental value $\Delta = 0.7$ eV [2] lies between these values. For comparison, the value of Δ inferred from the results by Deeth *et al* [19] and Larsson and Connolly [20] on CrF$_6^{3-}$ are equal to 1.2 eV and 1.1 eV. respectively. Also from the work of Larsson and Connolly, the value of Δ for different complexes can be derived. As a main trend, all the values are not far from 1 eV but they increase a little as far as the nominal charge of the central cation increases. Thus, for a complex such as MnF$_6^{4-}$, Δ is calculated to be equal to 1.6 eV [20]. This trend is in accord with experimental results [21].

If we accept that the oscillator strength of an $|i\rangle \rightarrow |f\rangle$ CT excitation is enhanced when both $|i\rangle$ and $|f\rangle$ involve σ orbitals, then the two transitions t$_{1u}(\sigma - \pi)$ ↓→ e$_g^*$ ↓ and t$_{1u}(\sigma + \pi)$ ↓→ e$_g^*$ ↓ could also be seen in the experimental spectrum. The results given in tables 1 and 2 indicate that the latter transition would be placed in the 11–13 eV

region. The separation from the $t_{1u}(\sigma + \pi) \uparrow \rightarrow e_g \uparrow$ transition reflects the effects of spin pairing in the 3d subshell and would be equal to $4D$. Therefore, as band C in figure 1 has a band width $W_C = 1.5$ eV with a peak of $E_C = 12$ eV, it could include the two transitions $t_{1u}(\sigma - \pi) \downarrow \rightarrow e_g \downarrow$ and $t_{1u}(\sigma + \pi) \downarrow \rightarrow e_g \downarrow$ but without further resolution. In other words, band C can also be related to CT transitions of CrF_6^{3-} at variance with the 3d $\rightarrow$ 4s assignment proposed by de Viry *et al* [2]. By contrast, the broader band D peaked at about 15 eV can hardly be ascribed to any CT transition in view of the present analysis.

It is worth noting that the present insight into CT bands associated with CrF_6^{3-} is consistent with the results obtained for other complexes embedded in ionic lattices [22, 23]. For instance, in the case of $NiCl_6^{4-}$ and $CuCl_6^{4-}$ the CT spectrum is composed of only two bands separated by 1 eV. As in this case the $\gamma_L \uparrow \rightarrow e_g^* \uparrow$ transitions are forbidden by the Pauli principle, the two observed transitions are assigned to $\gamma_L \downarrow \rightarrow e_g^* \downarrow$ where γ_L is $t_{1u}(\sigma - \pi)$ or $t_{1u}(\sigma + \pi)$. No signal of the $t_{2u} \downarrow \rightarrow e_g \downarrow$ transition is seen in the experimental spectra [22, 23] corresponding to $NiCl_6^{4-}$. In cases such as $CoCl_6^{4-}$ and $FeCl_6^{4-}$ a new band associated with the $t_{1u}(\sigma - \pi) \downarrow \rightarrow t_{2g} \downarrow$ transition has also been reported. The intensity of this transition (which in these cases is well separated form the $t_{1u}(\sigma - \pi) \downarrow \rightarrow e_g \downarrow$ transition by an energy of $10Dq$) is, however, smaller than that corresponding to transitions $t_{1u}(x) \downarrow \rightarrow e_g \downarrow$ $(x = \sigma - \pi; \sigma + \pi)$.

2.2. Sensitivity of charge-transfer transitions to variations in the metal–ligand distance R

Both the SCCEH and the MS–Xα calculations indicate (tables 1 and 2) that the two first CT energies seen in the spectrum of figure 1 (denoted as E_A and E_B, respectively) are very sensitive to changes in the Cr^{3+}–F^- distance.

Such sensitivity is measured through $\partial E/\partial R$. From the results collected in tables 1 and 2, $\partial E/\partial R$ exhibits values close to -200 meV pm^{-1} for both $t_{1u}(x) \uparrow \rightarrow e_g \uparrow$ $(x = \sigma - \pi$ or $\sigma + \pi)$ transitions.

As $W = 0.7$ eV for bands A and B, these results indicate that variations δR (induced by hydrostatic or chemical pressures) down to $(\delta R)_{min} \simeq 0.2$ pm can be detected through the maxima of such CT bands. Similar $(\delta R)_{min}$-values are reached using the CT bands of some Cu^{2+} complexes [3, 4]. As regards the transitions $t_{1u}(\sigma - \pi) \downarrow \rightarrow t_{2g}^* \downarrow$, the results collected in tables 1 and 2 show that $\partial E/\partial R$ is close to -140 meV pm^{-1} and thus somewhat smaller than the value corresponding to transition A where the electron jumps to an e_g^* orbital.

To understand the different $\partial E/\partial R$-values displayed by the $t_{1u}(\sigma - \pi) \uparrow \rightarrow e_g^* \uparrow$ and $t_{1u}(\sigma - \pi) \downarrow \rightarrow t_{2g}^* \downarrow$ transitions, the analysis made in [4] can be used. It was shown there that the R dependence of the separation between the *centre of gravity* of the t_{2g}^* and e_g^* levels and a ligand level is mainly governed by $\partial(V_M - V_L)/\partial R$ where

$$V_M = +6e^2/R$$
$$V_L = -\frac{e^2}{R}\left(Q - \frac{4}{\sqrt{2}} - \frac{1}{2}\right). \tag{3}$$

V_M is the electrostatic potential seen by an electron placed on the central cation due to the ligands, assuming initially that the ligand charge is just $-e$. V_L is the electrostatic potential for an electron situated on a ligand and Q is the total charge on the central cation, which is always smaller than the free-ion charge because of bonding. Taking the charge $Q = 1.5$, it is found that $\partial(V_M - V_L)/\partial R = -170$ meV pm^{-1}. To explain the different $\partial E/\partial R$-values displayed by the $t_{1u}(\sigma - \pi) \uparrow \rightarrow e_g^* \uparrow$ and $t_{1u}(\sigma - \pi) \downarrow \rightarrow t_{2g}^* \downarrow$ transitions we have to take into account the effects of chemical bonding leading to the $10Dq$ splitting, which is also

very sensitive to R changes. Therefore, $\partial E/\partial R$ can be written as

$$
\begin{aligned}
\frac{\partial E}{\partial R} &\simeq \frac{\partial (V_M - V_L)}{\partial R} + 6\frac{\partial Dq}{\partial R} && \text{for } t_{1u}(\sigma - \pi) \uparrow \rightarrow e_g^* \uparrow \\
\frac{\partial E}{\partial R} &\simeq \frac{\partial (V_M - V_L)}{\partial R} - 4\frac{\partial Dq}{\partial R} && \text{for } t_{1u}(\sigma - \pi) \downarrow \rightarrow t_{2g}^* \downarrow .
\end{aligned}
\tag{4}
$$

Thus the difference between the mentioned $\partial E/\partial R$-values should mainly reflect $\partial(10Dq)/\partial R = -n10Dq/R$ with $n \simeq 5$ which is just equal to about -50 meV pm^{-1} in the present case [26].

Indirect evidence of the sensitivity of CT transitions to variations in R can be obtained from the shift Δ_T experienced on warming from 10 K to room temperature. For the more intense band B, such a shift $\Delta_T = -0.2 \pm 0.1$ eV. This *red* shift can thus be qualitatively related to a higher R-value induced by thermal expansion effects.

It is worth noting, however, that such a shift is not only related to the referred thermal expansion effects. In fact, using thermodynamics arguments [24, 25], a quantity such as $(\partial E/\partial T)_p$ where E is the energy of a given optical transition is just given by

$$
\left(\frac{\partial E}{\partial T}\right)_p = \left(\frac{\partial E}{\partial V}\right)_T \left(\frac{\partial V}{\partial T}\right)_p + \left(\frac{\partial E}{\partial T}\right)_V .
\tag{5}
$$

In the present case the first term comes from thermal expansion effects and can simply be written as $(\partial E/\partial R)_T \alpha R$. Assuming that $\alpha = 2 \times 10^{-5}$ K^{-1} and taking $(\partial E/\partial R)_T = -200$ meV this contribution alone would lead to a shift close to -0.15 eV which is of the same order as the experimental value [2]. In a case such as RbMnF₃ it has been clearly demonstrated [25] that $(\partial E/\partial T)_V$ has the same sign and a similar value to the first term in (5).

2.3. Analysis of the band width

As pointed out very recently [26], the quantity $\partial E/\partial R$ related to the energy E of a given transition plays a crucial role in understanding the microscopic origin of optical parameters such as the associated band width or Stokes shift. As regards a band width corresponding to a complex such as CrF$_6^{3-}$ embedded in a host lattice, it is essentially determined by the linear electron–phonon coupling with vibrational modes of the complex. Let us designate by S_i the Huang–Rhys factor corresponding to a vibrational model whose frequency is $\omega_i/2\pi$. Then the band width at $T = 0$ K is given by [27]

$$
\begin{aligned}
W &= 2.36\sqrt{M_2} \\
M_2 &= \sum_i (\hbar\omega_i)^2 S_i .
\end{aligned}
\tag{6}
$$

For an octahedral complex there is only one symmetric mode A$_{1g}$, which always gives a contribution to W. Let us designate by ω_a and S_a the angular frequency and the Huang–Rhys factor, respectively, associated with such a mode. From (6) we find that

$$
W \geqslant W_a = 2.36\sqrt{S_a}\hbar\omega_a .
\tag{7}
$$

The Huang–Rhys factor S_a of an MX$_6$ complex is strongly related to $\partial E/\partial R$ through the expression [26]

$$
S_a = \frac{1}{12 M_L \hbar \omega_a^3} \left(\frac{\partial E}{\partial R}\right)^2
\tag{8}
$$

where M_L is the ligand mass.

From the results derived in section 2.2 for *both* band A and band B, it can be seen that $\partial E/\partial R \simeq -200$ meV pm^{-1}. As regards ω_a a value $\hbar\omega_a = 70$ meV can be used from the experimental information gathered [12–15] in the low-temperature $^4T_{2g} \rightarrow {}^4A_{2g}$ emission spectra of CrF_6^{3-}. Using both values and equation (8), it is found that $S_a = 20$. This value is thus certainly much larger than $S_a \simeq 1.4$ derived for the $^4T_{2g} \rightarrow {}^4A_{2g}$ crystal-field transition. This strong difference reflects the quite different values of $(\partial E/\partial R)$ in the two transitions because $\partial E/\partial R$ for the $^4A_{2g} \rightarrow {}^4T_{2g}$ transition of CrF_6^{3-} has been derived [26, 28] to be close to 50 meV pm^{-1}. Furthermore, the value $S_a = 20$ helps in understanding why no vibrational structure is observed [2] in the low-temperature CT spectra while rich vibrational progressions are observed in the corresponding crystal-field bands, where electron–phonon coupling is much weaker [12–15]. The value $S_a = 20$ leads to a band width $W_a = 0.7$ eV which is just equal to the experimental band width W displayed by bands A and B. By contrast, for the $t_{1u}(\sigma - \pi) \downarrow \rightarrow t_{2g}^* \downarrow$ transition, $\partial E/\partial R$ is calculated to be -140 meV pm^{-1}, and thus S_a and W_a should be equal to 10 and 0.5 eV, respectively. This analysis of the band width provides further support for the proposed assignment and, at the same time, allows one to gain a better insight into the microscopic origin of the band width corresponding to CT transitions. As an important result, the band width of CT bands appears to be essentially determined by the electron–phonon coupling with the symmetric A_{1g} mode. This situation is thus different from that encountered in the case of a crystal-field transition such as $^4A_{2g} \rightarrow {}^4T_{2g}$ of CrX_6^{3-} complexes (X = F, Cl or Br) where the Jahn–Teller mode E_g also plays an important role [9, 12–14, 26, 29].

3. Final comments

Through the present calculations of energy maxima and band widths, it has been possible to clarify which bands of the spectrum depicted in figure 1 can be ascribed to CT transitions of the CrF_6^{3-} complex and what is their most likely assignment. The results are compatible with the findings for other 3d complexes where the more intense CT bands involve $|i\rangle \rightarrow |f\rangle$ jumps where both $|i\rangle$ and $|f\rangle$ are σ orbitals [22, 23, 30].

In systems such as $NiCl_6^{4-}$ or $CuCl_6^{4-}$ the CT spectrum is composed of a doublet [22, 23]. By contrast, in the present case, four CT transitions are probably involved. This reflects the *two* possible values ($S' = 2$ and $S' = 1$) of the spin S' associated with the 3d subshell in the $t_{2g}^{*3}e_g^*$ configuration of CrF_6^{3-}. In contrast, no multiplet structure can appear in $NiCl_6^{4-}$ where the only possible value is $S' = 1/2$.

Aside from relating the strong $E(R)$ dependence to the experimental band width, the present results shed some light on possible luminescence from CT states *directly* to the ground state. In fact, if $S_a = 20, \hbar\omega_a = 70$ meV, the Stokes shift E_s would be *at least* equal to $E_{sa} = 2S_a\hbar\omega_a = 2.8$ eV and thus the emission maxima corresponding to peak A in figure 1 should be located at 5.2 eV. This figure has to be compared with the peak energies associated with the $^4T_{2g}(t_{2g}^{*2}e_g^*)$, $^4T_{1g}(t_{2g}^{*2}e_g^*)$ and $^4T_{1g}(t_{2g}^*e_g^{*2})$ crystal-field excitation bands [2] placed at 2.0 eV, 2.8 eV and 4.4 eV, respectively. Thus the closeness of a crystal-field excitation to the energy of the relaxed CT state clearly favours quenching of the direct luminescence while only that coming from the first excited state (reached after a cascade of non-radiative processes) is allowed. It is worth noting that, in $Al_2O_3 : Ti^{4+}$, the luminescence associated with the first CT band has been clearly observed [31] because Ti^{4+} is a closed shell and thus no crystal-field-like excitations can exist. The measured [31] Stokes shift ($E_s \simeq 2.5$ eV) is certainly much higher than that usually associated with crystal-field bands [26] but at the same time comparable with the value calculated for CrF_6^{3-}.

The present ideas can be useful for understanding the experimental features associated with the CT transitions of other systems. For instance, in recent work [30, 31] on $Al_2O_3 : Ti^{4+}$, two CT peaks located at 5.6 eV and 6.8 eV are observed which can be reasonably assigned to $t_{1u}(\sigma - \pi) \uparrow \rightarrow e_g^* \uparrow$ and $t_{1u}(\sigma + \pi) \uparrow \rightarrow e_g^* \uparrow$. In fact, if the first is assigned to $t_{1u}^*(\sigma - \pi) \uparrow \rightarrow t_{2g}^* \uparrow$ as in [31], it would imply that $10Dq = 1.2$ eV. However, $10Dq$ turns out to be higher than 2.5 eV for complexes of tetravalent 3d ions [32]. Moreover, the band width $W \simeq 0.7$ eV corresponding to the $t_{1u}(\sigma - \pi) \uparrow \rightarrow e_g^* \uparrow$ band and the corresponding Stokes shift $E_s = 2.5$ eV can again reasonably be explained essentially through a coupling with the A_{1g} mode and $S_a \simeq 16$, $\hbar\omega_a \simeq 80$ meV. For comparison in a complex such as TiF_6^{2-} it has been measured [33] to be $\hbar\omega_a = 77$ meV.

Following the analysis made in this work, the Huang–Rhys factor S_a, corresponding to a $\gamma_L \rightarrow t_{2g}^*$ transition can be significantly smaller than that corresponding to $\gamma_L \rightarrow e_g^*$. This idea can be helpful in explaining the observation of vibrational progressions involving the A_{1g} mode in the assigned $t_{1u}(\sigma - \pi) \downarrow \rightarrow t_{2g}^* \downarrow$ transition of $Cs_2NaYCl_6 : Fe^{3+}$ where [34] a value $S \simeq 8$ can be derived.

Although the present results support the statement that bands A, B and C of figure 1 come from CT excitations of CrF_6^{3-}, it is also true that the gap, corresponding to the $Na_3In_2Li_3Fe_{12}$ host lattice, has not yet been measured [35]. However, the optical absorption spectrum of $CrCl_3$ recently reported [36] sheds some light on this problem. In fact it is shown there that the first CT peak appears at about 5 eV. This value is thus consistent with the present analysis on the experimental results of $Na_2In_2Li_3F_{12} : Cr^{3+}$ and Jorgensen's optical electronegativity scale. The gap in $CrCl_3$ is visible in the optical spectrum at about 10 eV. On the other hand, other excitations which could be similar to band C in figure 1 are observed at about 7 eV in the optical absorption spectrum of $CrCl_3$. Therefore, the possible assignment of the feature around 15 eV in figure 1 as partially involving a transfer from the host lattice band gap, excitation to Cr^{3+} cannot yet be ruled out.

Although the present analysis points out that the band width of CT transitions can mainly be explained by considering *only* the coupling with the symmetric mode of the complex, further work is required to elucidate why the coupling with the Jahn–Teller mode E_g is certainly less important than for the $^4A_{2g} \rightarrow {}^4T_{2g}$ crystal-field transition of CrX_6^{3-} complexes (X = F, Cl or Br). Research in this direction is currently under way.

Acknowledgments

References

[1] Jørgensen C K 1962 *Solid State Physics* vol 13 (New York: Academic) p 375; 1970 *Prog. Inorg. Chem.* **12** 101
[2] de Viry D, Casalboni M, Palumno M and Zema N 1990 *Solid State Commun.* **76** 1051
[3] Breñosa A G, Moreno M, Rodríguez F and Couzi M 1991 *Phys. Rev.* B **44** 9859
[4] Aramburu J A , Moreno M and Barriuso M T 1992 *J. Phys.: Condens. Matter* **4** 9089
[5] Norman J G 1976 *Mol. Phys.* **31** 1191
[6] Valiente R, Aramburu J A, Barriuso M T and Moreno M 1994 *J. Phys.: Condens. Matter* **6** 4515
[7] Barriuso M T, Aramburu J A, Daul C and Moreno M 1996 *Int. J. Quant. Chem.* at press
[8] Luaña V, Bermejo M, Florez M, Recio J M and Pueyo L 1989 *J. Chem. Phys.* **90** 6409

[9]	Woods A M, Sinkovits R S, Charpie J C, Huang W L, Bartram R H and Rossi A R 1993 *J. Phys. Chem. Solids* **54** 543

[10]	Tressaud A private communication

[11]	de Viry D, Denis J P, Tercier N and Blanzat B 1987 *Solid State Commun.* **63** 1183

[12]	Ferguson J, Guggenheim H J and Wood D L 1971 *J. Chem. Phys.* **54** 504

[13]	Payne S A, Chase L L and Wilke G D 1989 *J. Lumin.* **44** 167

[14]	Marco de Lucas C, Rodríguez F, Dance J M, Moreno M and Tressaud A 1991 *J. Lumin.* **48–9** 553

[15]	Villacampa B, Casas González J, Alcalá R and Alonso P J 1991 *J. Phys.: Condens. Matter* **3** 8281

[16]	Barandiarán Z and Pueyo L 1984 *J. Chem. Phys.* **80** 1597

[17]	Rodríguez F and Moreno M 1986 *J. Chem. Phys.* **84** 692

[18]	Ballhausen C J 1962 *Introduction to Ligand Field Theory* (New York: McGraw Hill)

[19]	Deeth R J, Figgis B N and Ogden M J 1988 *Chem. Phys.* **121** 115

[20]	Larsson S and Connolly J W D 1974 *J. Chem. Phys.* **60** 1514

[21]	Moreno M 1979 *Solid State Commun.* **29** 653

[22]	Hirako S and Onaka R 1982 *J. Phys. Soc. Japan* **51** 1255

[23]	Simonetti J and McClure D S 1979 *J. Chem. Phys.* **71** 795

[24]	Walsh W M, Jeener J and Bloembergen N 1965 *Phys. Rev.* A **139** 1338

[25]	Rodríguez F, Moreno M, Dance J M and Tressaud A 1989 *Solid State Commun.* **69** 67

[26]	Moreno M, Barriuso M T and Aramburu J A 1992 *J. Phys.: Condens. Matter* **4** 9481; 1995 *J. Phys.: Condens. Matter* **7** 1749

[27]	Fitchen D B 1968 *Physics of Color Centres* ed B Fowler (New York: Academic) p 263

[28]	Dolan J F, Rinzler A G, Kappers L A and Bartram R H 1992 *J. Phys. Chem. Solids* **53** 905

[29]	Knochenmuss R, Reber C, Rajasekharan M V and Güdel H U 1983 *J. Chem. Phys.* **85** 4280

[30]	Desjardins S R, Penfield K W, Cohen S L, Musselman R L and Solomon E J 1983 *J. Am. Chem. Soc.* **105** 4590

[31]	Wong W C, McClure D S, Basum S A and Kokbta M R 1995 *Phys. Rev.* B **51** 5682

[32]	Donegan J F, Glynn T J, Imbusch G F and Remeika J P 1986 *J. Lumin.* **36** 93

[33]	Nakamoto K 1986 *Infrared and Raman Spectra of Inorganic and Coordination Compounds* (New York: Wiley)

[34]	Neuenschwander K, Güdel H U, Collingwood J C and Schatz P 1983 *Inorg. Chem.* **22** 1712

[35]	Casalboni M private communication

[36]	Pollini I 1994 *Phys. Rev.* B **50** 2095